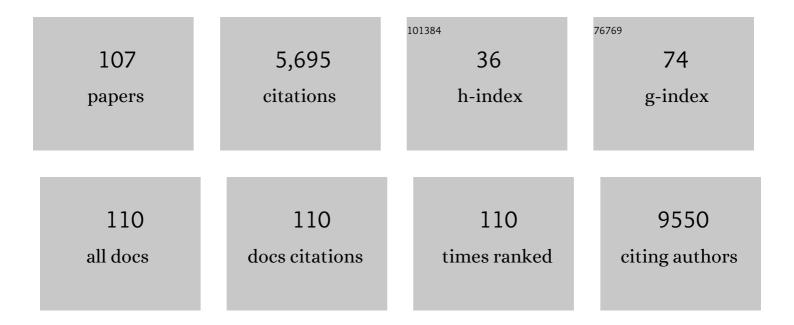
List of Publications by Year in descending order

Source: https://exaly.com/author-pdf/8461586/publications.pdf Version: 2024-02-01



#	Article	IF	CITATIONS
1	Size Control of Gold Nanocrystals in Citrate Reduction:  The Third Role of Citrate. Journal of the American Chemical Society, 2007, 129, 13939-13948.	6.6	1,149
2	Shape Control of Silver Nanoparticles by Stepwise Citrate Reduction. Journal of Physical Chemistry C, 2009, 113, 6573-6576.	1.5	291
3	Cleaning of Oil Fouling with Water Enabled by Zwitterionic Polyelectrolyte Coatings: Overcoming the Imperative Challenge of Oil–Water Separation Membranes. ACS Nano, 2015, 9, 9188-9198.	7.3	287
4	A Simple Route for Highly Luminescent Quaternary Cu-Zn-In-S Nanocrystal Emitters. Chemistry of Materials, 2011, 23, 3357-3361.	3.2	229
5	Improved photocatalytic activity of Sn4+ doped TiO2 nanoparticulate films prepared by plasma-enhanced chemical vapor deposition. New Journal of Chemistry, 2004, 28, 218.	1.4	212
6	Synthesis of water-soluble ZnS : Mn2+ nanocrystals by using mercaptopropionic acid as stabilizer. Journal of Materials Chemistry, 2003, 13, 1853.	6.7	210
7	Tumor Microenvironmentâ€Triggered Aggregation of Antiphagocytosis ^{99m} Tc‣abeled Fe ₃ O ₄ Nanoprobes for Enhanced Tumor Imaging In Vivo. Advanced Materials, 2017, 29, 1701095.	11.1	162
8	Small is Smarter: Nano MRI Contrast Agents – Advantages and Recent Achievements. Small, 2016, 12, 556-576.	5.2	147
9	Unraveling the Growth Mechanism of Silica Particles in the Stöber Method: In Situ Seeded Growth Model. Langmuir, 2017, 33, 5879-5890.	1.6	136
10	Extraordinarily Durable Graphdiyne-Supported Electrocatalyst with High Activity for Hydrogen Production at All Values of pH. ACS Applied Materials & Interfaces, 2016, 8, 31083-31091.	4.0	125
11	Synthesis of Triangular Silver Nanoprisms by Stepwise Reduction of Sodium Borohydride and Trisodium Citrate. Journal of Physical Chemistry C, 2010, 114, 2070-2074.	1.5	123
12	Formation and Stability of Gold Nanoflowers by the Seeding Approach: The Effect of Intraparticle Ripening. Journal of Physical Chemistry C, 2009, 113, 16645-16651.	1.5	122
13	Syntheses and Characterization of Nearly Monodispersed, Size-Tunable Silver Nanoparticles over a Wide Size Range of 7–200 nm by Tannic Acid Reduction. Langmuir, 2014, 30, 3876-3882.	1.6	112
14	Single Crystalline Submicrotubes from Small Organic Molecules. Chemistry of Materials, 2005, 17, 6430-6435.	3.2	110
15	Structure and Phase Transition Behavior of Sn ⁴⁺ -Doped TiO ₂ Nanoparticles. Journal of Physical Chemistry C, 2009, 113, 18121-18124.	1.5	110
16	Dot–Wire–Platelet–Cube: Step Growth and Structural Transformations in CsPbBr ₃ Perovskite Nanocrystals. ACS Energy Letters, 2018, 3, 2014-2020.	8.8	106
17	Protease-Activated Ratiometric Fluorescent Probe for pH Mapping of Malignant Tumors. ACS Nano, 2015, 9, 3199-3205.	7.3	102
18	From Achiral Molecular Components to Chiral Supermolecules and Supercoil Self-Assembly. Chemistry - A European Journal, 1999, 5, 1144-1149.	1.7	94

WENSHENG YANG

38

#	Article	IF	CITATIONS
19	Non-injection gram-scale synthesis of cesium lead halide perovskite quantum dots with controllable size and composition. Nano Research, 2016, 9, 1994-2006.	5.8	93
20	Effect of ultrasonic treatment on dispersibility of Fe3O4 nanoparticles and synthesis of multi-core Fe3O4/SiO2 core/shell nanoparticles. Journal of Materials Chemistry, 2005, 15, 4252.	6.7	82
21	Preparation of Fe3O4/polystyrene composite particles from monolayer oleic acid modified Fe3O4 nanoparticles via miniemulsion polymerization. Journal of Nanoparticle Research, 2009, 11, 289-296.	0.8	78
22	An ambipolar organic field-effect transistor based on an AIE-active single crystal with a high mobility level of 2.0 cm ² V ^{â^'1} s ^{â^'1} . Chemical Communications, 2016, 52, 2370-2373.	2.2	73
23	2,4,5-Triphenylimidazole Nanowires with Fluorescence Narrowing Spectra Prepared through the Adsorbent-Assisted Physical Vapor Deposition Method. Chemistry of Materials, 2006, 18, 2302-2306.	3.2	71
24	Aqueous Synthesis of ZnSe Nanocrystals by Using Glutathione As Ligand: The pH-Mediated Coordination of Zn ²⁺ with Glutathione. Journal of Physical Chemistry C, 2010, 114, 11087-11091.	1.5	69
25	Colloidal preparation and electrocatalytic hydrogen production of MoS2and WS2nanosheets with controllable lateral sizes and layer numbers. Nanoscale, 2016, 8, 15262-15272.	2.8	64
26	Highly magnetizable superparamagnetic iron oxide nanoparticles embedded mesoporous silica spheres and their application for efficient recovery of DNA from agarose gel. Journal of Materials Chemistry, 2009, 19, 1811.	6.7	62
27	Tuning the Emission Properties of Ru(phen) ₃ ²⁺ Doped Silica Nanoparticles by Changing the Addition Time of the Dye during the Stöber Process. Langmuir, 2010, 26, 6657-6662.	1.6	51
28	Highly Efficient Multiâ€Resonance Thermally Activated Delayed Fluorescence Material with a Narrow Full Width at Halfâ€Maximum of 0.14ÂeV. Small, 2022, 18, e2106462.	5.2	50
29	Preparation of nearly monodispersed Fe3O4/SiO2 composite particles from aggregates of Fe3O4 nanoparticles. Journal of Materials Chemistry, 2011, 21, 15352.	6.7	49
30	Upconversion luminescence nanoparticles-based lateral flow immunochromatographic assay for cephalexin detection. Journal of Materials Chemistry C, 2014, 2, 9637-9642.	2.7	48
31	Synthesis of Monodisperse, Highly Emissive, and Size-Tunable Cd3P2 Nanocrystals. Chemistry of Materials, 2010, 22, 3820-3822.	3.2	47
32	Large-scale synthesis of single-source, thermally stable, and dual-emissive Mn-doped Zn–Cu–In–S nanocrystals for bright white light-emitting diodes. Nano Research, 2015, 8, 3316-3331.	5.8	46
33	Bioinspired 1D Superparamagnetic Magnetite Arrays with Magnetic Field Perception. Advanced Materials, 2016, 28, 6952-6958.	11.1	45
34	Color Tunable Selfâ€Trapped Emissions from Leadâ€Free All Inorganic IAâ€IB Bimetallic Halides Csâ€Agâ€X (X =	Cl,) Ţi ET	Qq0_0 0 rgBT
35	Gold Nanoparticle-Based Facile Detection of Human Serum Albumin and Its Application as an INHIBIT Logic Gate. ACS Applied Materials & Interfaces, 2015, 7, 8990-8998.	4.0	43

pH-dependent aggregation of citrate-capped Au nanoparticles induced by Cu2+ ions: The competition effect of hydroxyl groups with the carboxyl groups. Colloids and Surfaces A: Physicochemical and 2.3 Engineering Aspects, 2009, 346, 216-220.

#	Article	IF	CITATIONS
37	pH-Dependent Aggregation of Histidine-Functionalized Au Nanoparticles Induced by Fe ³⁺ Ions. Journal of Physical Chemistry C, 2008, 112, 3267-3271.	1.5	37
38	Synthesis of donor–acceptor molecules based on isoxazolones for investigation of their nonlinear optical properties. Journal of Materials Chemistry C, 2013, 1, 5694.	2.7	36
39	Synthesis of robust water-soluble ZnS:Mn/SiO2 core/shell nanoparticles. Journal of Nanoparticle Research, 2008, 10, 653-658.	0.8	29
40	Incorporating anionic dyes into silicananoparticles by using a cationic polyelectrolyte as a bridge. Journal of Materials Chemistry, 2011, 21, 1147-1152.	6.7	29
41	Aggregation-Enhanced Emission of Gold Nanoclusters Induced by Serum Albumin and Its Application to Protein Detection and Fabrication of Molecular Logic Gates. ACS Omega, 2018, 3, 12763-12769.	1.6	28
42	Controlling the Interface Areas of Organic/Inorganic Semiconductor Heterojunction Nanowires for High-Performance Diodes. ACS Applied Materials & Interfaces, 2016, 8, 21563-21569.	4.0	26
43	Citrate-Regulated Surface Morphology of SiO ₂ @Au Particles To Control the Surface Plasmonic Properties. Journal of Physical Chemistry C, 2016, 120, 377-385.	1.5	25
44	Rationalized Fabrication of Structure-Tailored Multishelled Hollow Silica Spheres. Chemistry of Materials, 2019, 31, 7470-7477.	3.2	25
45	ICG@ZIF-8/PDA/Ag composites as chemo-photothermal antibacterial agents for efficient sterilization and enhanced wound disinfection. Journal of Materials Chemistry B, 2021, 9, 9961-9970.	2.9	24
46	Single-phase dual emissive Cu:CdS–ZnSe core–shell nanocrystals with "zero self-absorption―and their application in white light emitting diodes. Journal of Materials Chemistry C, 2015, 3, 3614-3622.	2.7	23
47	Glutathione-facilitated design and fabrication of gold nanoparticle-based logic gates and keypad lock. Nanoscale, 2014, 6, 8300-8305.	2.8	22
48	Bifunctional Superparticles Achieved by Assembling Fluorescent CuInS2@ZnS Quantum Dots and Amphibious Fe3O4Nanocrystals. Journal of Physical Chemistry C, 2013, 117, 21014-21020.	1.5	21
49	Size-selective separation of DNA fragments by using lysine-functionalized silica particles. Scientific Reports, 2016, 6, 22029.	1.6	20
50	One-pot synthesis of size-tunable hollow gold nanoshells via APTES-in-water suspension. Colloids and Surfaces A: Physicochemical and Engineering Aspects, 2016, 502, 6-12.	2.3	20
51	Optimizing the activity of Pd based catalysts towards room-temperature formic acid decomposition by Au alloying. Catalysis Science and Technology, 2019, 9, 588-592.	2.1	19
52	BiOl/Bi ₂ O ₂ CO ₃ Two-Dimensional Heteronanostructures with Boosting Charge Carrier Separation Behavior and Enhanced Visible-Light Photocatalytic Performance. Journal of Physical Chemistry C, 2020, 124, 20294-20308.	1.5	19
53	The effect of indium doping on the hydrogen evolution performance of g-C ₃ N ₄ based photocatalysts. New Journal of Chemistry, 2021, 45, 544-550.	1.4	19
54	Self-assembly of luminescent twisted fibers based on achiral quinacridone derivatives. Nano Research, 2009, 2, 493-499.	5.8	18

#	Article	IF	CITATIONS
55	CXC Chemokine Receptor 4 Antagonist Functionalized Renal Clearable Manganese-Doped Iron Oxide Nanoparticles for Active-Tumor-Targeting Magnetic Resonance Imaging-Guided Bio-Photothermal Therapy. ACS Applied Bio Materials, 2019, 2, 3613-3621.	2.3	18
56	High-purity gold nanocrystal dimers: scalable synthesis and size-dependent plasmonic and Raman enhancement. Chemical Science, 2014, 5, 311-323.	3.7	17
57	The effect of NaOH on lowering interfacial tension of oil/alkylbenzene sulfonates solution. RSC Advances, 2018, 8, 6169-6177.	1.7	17
58	Improved activity of immobilized horseradish peroxidase on gold nanoparticles in the presence of bovine serum albumin. Journal of Nanoparticle Research, 2013, 15, 1.	0.8	14
59	Colloidal silica assisted fabrication of N,O,S-tridoped porous carbon nanosheets with excellent oxygen reduction performance. Chemical Communications, 2018, 54, 4017-4020.	2.2	14
60	Promoting hydrogen evolution of a g-C ₃ N ₄ -based photocatalyst by indium and phosphorus co-doping. New Journal of Chemistry, 2021, 45, 7231-7238.	1.4	14
61	Mesoporous silica-coated superparamagnetic particles prepared by pseudomorphic transformation and their application in purification of plasmid DNA. Journal of Nanoparticle Research, 2011, 13, 6613-6620.	0.8	13
62	Controlling the Growth of Molecular Crystal Aggregates with Distinct Linear and Nonlinear Optical Properties. ACS Applied Materials & Interfaces, 2017, 9, 30862-30871.	4.0	13
63	Glutathione-Capped Au Nanoclusters Embedded in NaCl Crystals for White Light-Emitting Devices. ACS Applied Nano Materials, 2021, 4, 7486-7492.	2.4	13
64	Ultra-small nickel phosphide nanoparticles as a high-performance electrocatalyst for the hydrogen evolution reaction. RSC Advances, 2016, 6, 74895-74902.	1.7	12
65	Zero-dimensional plate-shaped copper halide crystals with green-yellow emissions. Materials Advances, 2021, 2, 3744-3751.	2.6	12
66	Theoretical design of two-dimensional carbon nitrides. Nanotechnology, 2020, 31, 495707.	1.3	11
67	Title is missing!. Journal of Nanoparticle Research, 2000, 2, 309-313.	0.8	10
68	Bandgap―and Radialâ€Positionâ€Đependent Mnâ€Doped Zn–Cu–In–S/ZnS Core/Shell Nanocrystals. ChemPhysChem, 2016, 17, 752-758.	1.0	10
69	Preparation of Gold/triblock Copolymer Composite Nanoparticles. Journal of Nanoparticle Research, 2000, 2, 381-385.	0.8	9
70	THE IN VIVO INVESTIGATION OF Fe3O4-NANOPARTICLES ACUTE TOXICITY IN MICE. Biomedical Engineering - Applications, Basis and Communications, 2012, 24, 229-235.	0.3	9
71	The coordination sites of phosphorothioate OligoG10 with Cd2+ and CdS nanoparticles. New Journal of Chemistry, 2003, 27, 823-826.	1.4	8
72	Exciton–Phonon Coupling and Low Energy Emission in 2D and Quasi-2D BA ₂ MA _{<i>n</i>–1} Pb _{<i>n</i>} I _{3<i>n</i>+1} Thin Films with Improved Phase Purity. Journal of Physical Chemistry Letters, 2021, 12, 12336-12344.	2.1	8

#	Article	IF	CITATIONS
73	Frontier orbital interactions of electron pushing and drawing substituents with ferrocenyl group. Science in China Series B: Chemistry, 1997, 40, 236-244.	0.8	7
74	cis-trans Driven organized reorientation of an azobenzene derivative monolayer at the liquid/graphite interface. New Journal of Chemistry, 2003, 27, 1463-1465.	1.4	7
75	Bovine serum albumin assisted preparation of ultra-stable gold nanoflowers and their selective Raman response to charged dyes. RSC Advances, 2019, 9, 28228-28233.	1.7	7
76	Histidine-directed formation of nearly monodispersed silver nanoflowers and their ultra-high peroxidase-like activity under physiological pH. Applied Surface Science, 2020, 532, 147457.	3.1	7
77	Aggregation behavior of amphiphilic D-ï€-A molecules bearing recognition group. Science in China Series B: Chemistry, 2000, 43, 555-560.	0.8	6
78	Polyelectrolyte-assisted preparation of gold nanocluster-doped silica particles with high incorporation efficiency and improved stability. Journal of Nanoparticle Research, 2017, 19, 1.	0.8	6
79	Luminescent metal clusters/barium sulfate composites for white light-emitting devices and anti-counterfeiting labels. RSC Advances, 2018, 8, 2866-2871.	1.7	6
80	Peptide modified manganese-doped iron oxide nanoparticles as a sensitive fluorescence nanosensor for non-invasive detection of trypsin activity <i>in vitro</i> and <i>in vivo</i> . RSC Advances, 2021, 11, 2213-2220.	1.7	6
81	Preparation of fractal-like silica particles based on Stöber method by using tetrabutylammonium hydroxide as co-catalyst. Colloids and Surfaces A: Physicochemical and Engineering Aspects, 2021, 626, 127091.	2.3	6
82	Phenanthroline method for quantitative determination of surface carboxyl groups on carboxylated polystyrene particles with high sensitivity. Surface and Interface Analysis, 2009, 41, 577-580.	0.8	5
83	Charge reversible gold nanoparticles for high efficient absorption and desorption of DNA. Journal of Nanoparticle Research, 2012, 14, 1.	0.8	5
84	Effects of Cu2+ on aggregation behavior of poly (l-Glutamic Acid)-functionalized gold nanoparticles. Journal of Nanoparticle Research, 2013, 15, 1.	0.8	5
85	Fabrication of Bovine Serum Albumin@Au Particles for Colorimetric Detection of Glutathione. ACS Applied Bio Materials, 2020, 3, 9109-9116.	2.3	5
86	Controlled growth of 2D ultrathin Ga ₂ O ₃ crystals on liquid metal. Nanoscale Advances, 2021, 3, 4411-4415.	2.2	5
87	Growth and Etching of Centimeter-Scale Self-Assembly Graphene–h-BN Super-Ordered Arrays: Implications for Integrated Electronic Devices. ACS Applied Nano Materials, 2022, 5, 774-781.	2.4	5
88	Ultrafast Photophysics of Multiple-Resonance Ultrapure Blue Emitters. Journal of Physical Chemistry B, 2022, 126, 2729-2739.	1.2	5
89	Confined Assembly of Colloidal Nanorod Superstructures by Locally Controlling Freeâ€Volume Entropy in Nonequilibrium Fluids. Advanced Materials, 2022, 34, e2202119.	11.1	5
90	Tuning Hybridized Local and Charge-Transfer Mixing for Efficient Hot-Exciton Emission with Improved Color Purity. Journal of Physical Chemistry Letters, 2022, 13, 6664-6673.	2.1	5

#	Article	IF	CITATIONS
91	Facile Synthesis, Enhanced Photostability, and Long-term Cellular Imaging of Bright Red Luminescent Organosilica Nanoparticles. ACS Applied Bio Materials, 2020, 3, 5438-5445.	2.3	4
92	Tetrabutylammonium bromide assisted preparation of monodispersed submicrometer silica particles. Colloids and Surfaces A: Physicochemical and Engineering Aspects, 2021, 614, 126171.	2.3	4
93	Cetyltrimethylammonium bromide promoted dispersing and incorporation of curcumin into silica particles in alkaline ethanol/water mixture. Colloids and Surfaces A: Physicochemical and Engineering Aspects, 2021, 624, 126789.	2.3	4
94	N-Doped Carbon Dots Embedded in Silica Nanoparticles with Multicolor Luminescence for Light-Emitting Devices. ACS Applied Nano Materials, 2021, 4, 13625-13632.	2.4	4
95	3-Aminopropyltriethoxysilane-directed formation of Au popcorns for colorimetric and SERS dual detection of cysteine. Colloids and Surfaces A: Physicochemical and Engineering Aspects, 2022, 647, 129033.	2.3	4
96	Potentialâ€induced Raman behavior of individual (<i>R</i>)â€diâ€2â€naphthylprolinol molecules on a Agâ€modified Ag electrode. Journal of Raman Spectroscopy, 2011, 42, 951-957.	1.2	3
97	Controllable growth of organic nanostructures from 0D to 1D with different optical properties. RSC Advances, 2015, 5, 100457-100463.	1.7	3
98	Phase Engineering of Hydrophobic Meso-Environments in Silica Particles for Technical Performance Enrichment. Langmuir, 2018, 34, 7428-7435.	1.6	3
99	Au Nanoflowers for Catalyzing and In Situ Surface-Enhanced Raman Spectroscopy Monitoring of the Dimerization of p-Aminothiophenol. ACS Omega, 2021, 6, 25720-25728.	1.6	3
100	Monoglycocalix[4]arene-based nanoparticles for tumor selective drug delivery <i>via</i> GLUT1 recognition of hyperglycolytic cancers. Organic and Biomolecular Chemistry, 2022, 20, 4884-4887.	1.5	3
101	Ï€-Ï€ interactions in the self-assembly of melamine and barbituric acid derivatives. Science in China Series B: Chemistry, 2001, 44, 478-485.	0.8	2
102	Animal heat activated cancer therapy by a traditional catalyst TiO2-Pd/graphene composites. Scientific Reports, 2020, 10, 15823.	1.6	2
103	Fabrication of prime number checkers based on colorimetric responses of gold nanoparticles. New Journal of Chemistry, 2019, 43, 8728-8734.	1.4	1
104	Efficient loading of curcumin into CTAB micelle-embedded silica particles for visualized pH detection. Colloids and Surfaces A: Physicochemical and Engineering Aspects, 2022, 637, 128250.	2.3	1
105	Ï€-Ï€ Interactions Directed Formation of A Self-assembled Nanofilament. Molecular Crystals and Liquid Crystals, 2001, 371, 91-94.	0.3	0
106	DNA-Templated Formation of Needle-like CdS Nanoparticles in Langmuir-Blodgett Film. Molecular Crystals and Liquid Crystals, 2001, 371, 49-52.	0.3	0
107	Histidine-directed formation of Ag octopods via pseudomorphic transformation of Ag2O. Materials Chemistry Frontiers, 2021, 5, 5478-5485.	3.2	0